by eight 80 km-long SMFs (see Fig. 2, (ii)) or nonzero dispersion shifted fibres (NZ-DSFs) (see Fig. 2, (iii)). All the EDFA modules in Fig. 2, (iv) consisted of two-stage EDFA and dispersion compensating fibre (DCF). The input power was set to be 0 dBm for both the SMF and NZ-DSF links, while it was reduced to –3 dBm for the SMF+DCF link. We used an additional EDFA module as a preamplifier in front of the demultiplexer, except in the case of the back-to-back experiment. The WDM signals were demultiplexed by using an AWG and sent to the OSNR monitoring module. The signal power incident on the monitoring module was set to be –15 dBm. We then measured the OSNRs in each fibre link for 10 h to investigate the effects of PMD and nonlinear birefringence. The total PMDs for the 640 km-long SMF, NZ-DSF, and SMF+DCF links were measured to be 1.32, 1.52, and 3.22 ps, respectively.

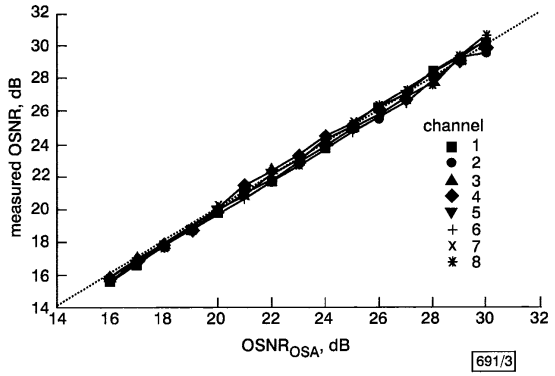

Fig. 3 *Measured OSNRs in back-to-back experiment*

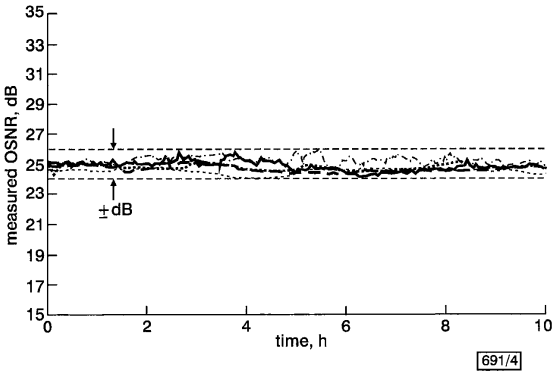

Fig. 4 *Measured OSNRs for 10 h operation in various fibre links (from Fig. 2)*

——— SMF (2.5 Gbit/s)
— — NZ-DSF (2.5 Gbit/s)
– – – – NZ-DSF (10 Gbit/s)
····· SMF + DCF (2.5 Gbit/s)
–·–·– SMF + DCF (10 Gbit/s)

Fig. 3 shows the performance of the proposed OSNR monitoring technique measured in the back-to-back experiment. The result shows that the measured OSNRs agree well with the values obtained by using an optical spectrum analyser (OSA) within ±0.3 dB for every channel. Fig. 4 shows the OSNRs measured by the proposed technique for 10 h in various fibre links. The proposed technique could measure the OSNRs with accuracy better than ±1 dB, regardless of the bit rates and/or types of 640 km-long fibre links. Thus, we concluded that the proposed technique could negate the deleterious effects of PMD and nonlinear birefringence effectively by including the ratio ε in the estimation of OSNRs.

Summary: We have proposed and demonstrated an improved version of the OSNR monitoring technique based on the polarisation-nulling method. This technique utilised an optical bandpass filter, in addition to the polarisation beam splitter, to negate the deleterious effects of PMD and nonlinear birefringence. The results show that the proposed technique could monitor the OSNR with accuracy better than ±1 dB, regardless of the bit rates, even when the transmission link had large PMD and low dispersion (thus, large nonlinear birefringence). Thus, we believe that the proposed technique could be used to monitor the OSNRs accurately even in the network with large PMD or nonlinear birefringence.

Acknowledgment: This work was supported in part by the NRL programme of MOST and ETRI.

18 May 2001
Electronics Letters Online No: 20010655
DOI: 10.1049/el:20010655

J.H. Lee and Y.C. Chung (*Korea Advanced Institute of Science and Technology, Department of Electrical Engineering, 373-1 Kusong-dong, Yusong-gu, Taejon 305-701, Korea*)

E-mail: ychung@ee.kaist.ac.kr

References

1 ASAHI, K., YAMASHITA, M., HOSOI, T., NAKAYA, K., and KONOSHI, C.: 'Optical performance monitor built into EDFA repeaters for WDM networks'. OFC '98, San Jose, CA, USA, 1998, Paper ThO2
2 SUZUKI, H., and TAKACHIO, N.: 'Optical signal quality monitor built into WDM linear repeaters using semiconductor arrayed waveguide grating filter monolithically integrated with eight photodiodes', *Electron. Lett.*, 1999, **35**, (10), pp. 836–837
3 LEE, J.H., JUNG, D.K., KIM, C.H., and CHUNG, Y.C.: 'OSNR monitoring technique using polarization-nulling method', *IEEE Photonics Technol. Lett.*, 2001, **12**, (1), pp. 88–90

High speed evanescently coupled *PIN* photodiodes for hybridisation on silicon platform optimised with genetic algorithm

L. Giraudet, J. Harari, V. Magnin, P. Pagnod, E. Boucherez, J. Decobert, J. Bonnet-Gamard, D. Carpentier, C. Jany, F. Blache and D. Decoster

Evanescently coupled photodiodes have been designed for hybridisation on an Si platform. Diluted multimode waveguides have been optimised with a genetic algorithm. High efficiency photodiodes at both 1.3 and 1.5 μm, with very low polarisation dependence, have been fabricated with low bias, 2.5 Gbit/s capability and high reliability.

Introduction: Low-cost packaging is essential for the development of present day optical fibre networks. Hybridisation on a silicon platform has been introduced as an alternative to high precision pigtailing of individual devices (lasers, photodiodes, etc.) or to complex, costly assemblies [1]. In particular, edge illuminated photodiodes have been studied [2, 3] for this purpose, using a direct illumination scheme. This scheme has some known impairments: input facet fabrication with junction passivation is difficult to achieve with high reliability [4, 5], and some compromise may be necessary with respect to low bias–high optical power operation.

Our work has focused on edge illuminated, evanescently coupled *PIN* photodiodes, since they allow the above impairments to be overcome: (i) passivation of planar junction is well established; (ii) passivation of the input facet is no longer an issue since it is not electrically active; and (iii) high optical power capability is known to be better than for direct illumination [6] due to diluted absorption of light resulting in lower carrier concentration in the junction.

High performance devices have been fabricated for 2.5 Gbit/s operation at –3 V, high responsivity and high reliability. Furthermore, the evanescent coupling scheme allows the integration of the dry etched waveguide input facet with antireflection coating deposition on-wafer, and V grooves for high precision cleaving. This results in very low cost, high performance *PIN* photodiodes suitable for hybridisation on an Si platform for 2.5 Gbit/s modules.

Photodiode design: A schematic diagram of the cross-section of the device is shown in Fig. 1. It is based on an original diluted multi-

mode input waveguide, followed by an evanescently coupled planar *PIN* photodiode. An adaptation layer is inserted in between to improve coupling efficiency to the diode, as demonstrated in previous work [7]. The use of a multimode input waveguide was dictated by the need for high coupling tolerances with cleaved or lensed fibres. The structure presented here was designed to achieve ±2 μm (–1 dB excess loss) fibre alignment tolerance, with 6 μm diameter fibre (at 1.55 μm). Furthermore, diluted waveguides are very efficient design tools, while keeping epitaxy very simple as only one material composition is used.

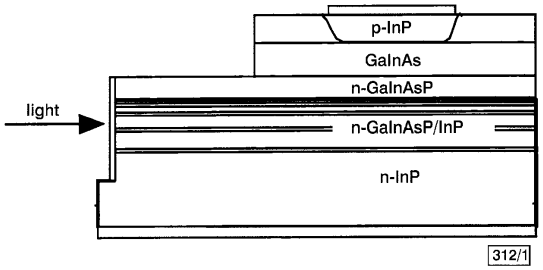

Fig. 1 *Schematic diagram of evanescent PIN photodiode, showing injected light on tilted etched facet*

The optimisation of such a structure using BPM could be very time consuming due to the numerous layers, and device dimensions such as input waveguide length and photodiode length. Furthermore, the targeted performances of the devices are also numerous: operation at both 1.3 and 1.55 μm wavelength range, low polarisation dependence and high coupling tolerances. Therefore a genetic algorithm, coupled to a two-dimensional BPM simulation tool, was required to optimise the structure, as described in [8]. Optimisation using different criteria is possible by using an appropriate fitness function, and a high performance structure was established. The structures should allow more than 90% efficiency at both wavelengths with almost no polarisation dependence for 150 μm-long diodes.

A 10° tilted dry etched input facet was also designed for low back reflection in the fibre, as allowed by the evanescent approach. In addition, a planar waveguide is used for the purpose of fabrication simplicity, and the photodiode is designed so that the *PIN* junction follows the light travel and mode expansion into the semiconductor structure (see Fig. 2).

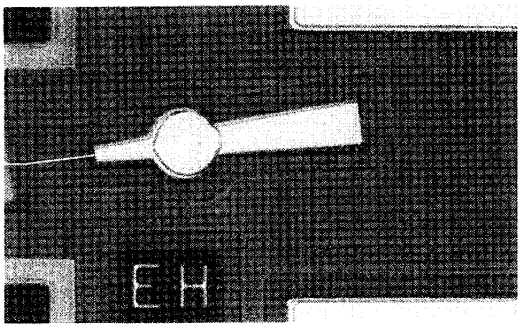

Fig. 2 *Photograph of fabricated device*

Light pass is indicated by white line. V-grooves are located each side of tilted facet

Fabrication: The structures are grown by MOCVD on *n*-InP substrates. After photodiode mesa formation down to the multimode waveguide top layer, zinc diffusion is performed through an SiNx mask for junction formation achieving high reliability. This is a major advantage of the evanescent illumination scheme compared to direct coupling. *P*-type ohmic contacts are then formed. The input facet is etched using vertical RIE, and an antireflection coating is deposited on wafer. No particular attention has to be paid to this coating since the input facet is completely passive, and junction passivation is already achieved. In addition, V-grooves are chemically etched to help precise cleaving in front of the input facet. This also helps further positioning on Si board and improves fibre coupling efficiency. A photograph of the device is shown in Fig. 2. The devices are fully functional at the wafer stage, allowing on-probe characterisation. No additional, usually costly, AR coating deposition needs to be performed. These advantages result in high reliability and low-cost fabrication technology.

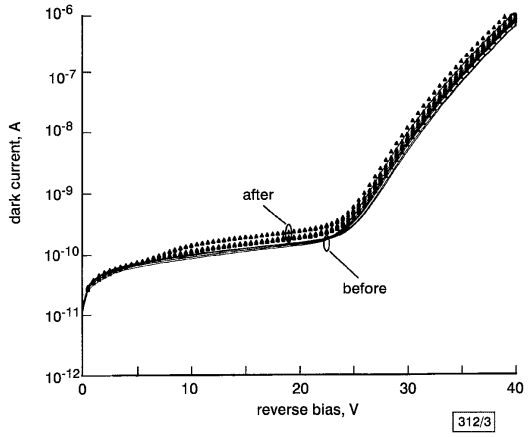

Fig. 3 *Room temperature dark current characteristics before and after burn-in test (1000 h at 200°C-10 V in ambient atmosphere)*

Results: Typical dark current characteristics are shown in Fig. 3, before and after a 200°C-10 V-168 h burn-in cycle. Very low dark current is achieved, close to 100 pA at –10 V, and no evolution is seen after burn-in test. This is due to the highly reliable planar junction.

Responsivity measurements were performed at both 1.3 and 1.55 μm using a lensed fibre (5.8 μm mode diameter at 1.55 μm). Responsivities as high as 0.91 A/W at 1.3 μm and 1.05 A/W at 1.55 μm are measured, with almost no polarisation dependence (much lower than 0.5 dB). The fibre alignment tolerances are ±1.9 μm at –1 dB. These results are in very close agreement with simulation. This shows the efficiency of the design, of the design tools, and of the fabrication technology. In particular, almost no degradation is seen from the use of the dry etched input facet with antireflection coating deposited on-wafer, and very high internal quantum efficiency is demonstrated.

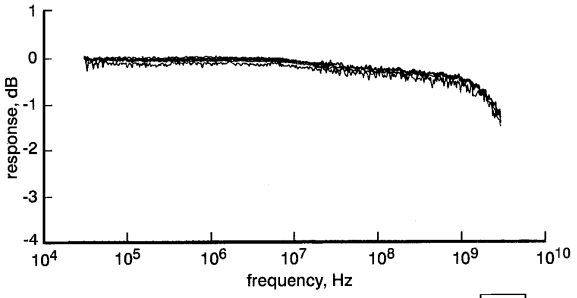

Fig. 4 *30 kHz–3 GHz frequency response of photodiode for optical power ranging from –12 to 0 dBm*

Applied reverse bias is –3 V

30 kHz to 3 GHz bandwidth measurements have been performed with optical power ranging from –12 to 0 dBm. This 0 dBm value is required for the back-to-back system test. Applied reverse bias was varied (–3 V to –10 V). As seen in Fig. 4, all bandwidths are well in excess of 3 GHz, and no dependence on optical power was seen even at –3 V. The devices are thus suitable for 2.5 Gbit/s operation.

Conclusion: High performance 2.5 Gbit/s *PIN* photodiodes have been designed and fabricated for hybridisation on an Si platform. The original design is based on multimode input waveguide with evanescent coupling. A very efficient genetic algorithm and BPM tool was used to optimise the structure and diode dimensions for 1.3 to 1.55 μm operation. The fabrication technology includes facet etching, antireflection coating and V grooves on-wafer, with a

high reliability *PIN* junction process. The 150 μm-long fabricated diodes show responsivities as high as 0.91 A/W at 1.3 μm and 1.05 A/W at 1.55 μm, almost no polarisation dependence, and ±1.9 μm –1 dB fibre alignment tolerances. Furthermore, they demonstrate very stable dark current during burn-in test with dark current in the 100 pA range, due to the planar junction. Bandwidths in excess of 3 GHz are measured at –3 V with no dependence on optical power up to 0 dBm. The devices are suitable for low-cost, silicon mother-board based, 2.5 Gbit/s modules.

26 April 2001
Electronics Letters Online No: 20010664
DOI: 10.1049/el:20010664

L. Giraudet, P. Pagnod, E. Boucherez, J. Decobert, J. Bonnet-Gamard, D. Carpentier, C. Jany and F. Blache (*Opto+, Groupement d'intérêt économique, Route de Nozay, 61460 Marcoussis, France*)

J. Harari, V. Magnin and D. Decoster (*IEMN, Avenue Poincaré, 59652 Villeneuve d'Ascq, France*)

References

1 FERNIER, B., ADAM, K., ARTIGUE, C., BARROU, T., GOTH, A., GRARD, E., JORG, W., KELLER, D., LAFRAGETTE, J.L., LESTRA, A., PAGNOD, P., RABARON, S., RAISANT, J.M., SCHERB, J., TOULLIER, D., TREGOAT, D., and REHM, W.: '1.3 μm low cost plastic module for 622 Mbit/s transmission at 85°C'. Proc ECOC'98, Madrid, Sept. 1998, pp. 445–446

2 AKATSU, Y., MURAMOTO, Y., KATO, K., IKEDA, M., UEKI, M., KOZEN, A., KUROSAKI, T., KAWANO, K., and YOSHIDA, J.: 'Long-wavelength multimode waveguide photodiodes suitable for hybrid optical module integrated with planar lightwave circuit', *Electron. Lett.*, 1995, **31**, (24), pp. 2098–2099

3 SHISHIKURA, M., NAKAMURA, H., TANAKA, S., MATSUOKA, Y., ONO, T., MIYAZAKI, T., and TSUJI, S.: 'High-responsivity low-dark-current InGaAlAs waveguide photodiode with a symmetric double-core for optical access networks', *Electron. Lett.*, 1996, **32**, (20), pp. 1882–1883

4 NAKAMURA, H., SHISHIKURA, M., TANAKA, S., MATSUOKA, Y., ONO, T., MIYAZAKI, T., and TSUJI, S.: 'High responsivity, low-dark-current, and high reliable operation of InGaAlAs waveguide photodiodes for optical hybrid integration', *IEICE Trans. Electron.*, 1997, **E80-C**, (1), pp. 41–46

5 MAWATARI, H., FUKUDA, M., KATO, K., TAKESHITA, T., YUDA, M., KOZEN, A., and TOBA, H.: 'Reliability of planar waveguide photodiodes for optical subscriber systems', *J. Lightwave Technol.*, 1998, **16**, (12), pp. 2428–2429

6 TAKEUCHI, T., NAKATA, T., MAKITA, K., and YAMAGUCHI, M.: 'High-speed, high-power and high efficiency photodiode with evanescently coupled graded-index waveguide', *Electron. Lett.*, 2000, **36**, (11), pp. 972–978

7 GIRAUDET, L., BANFI, F., DEMIGUEL, S., and HERVE-GRUYER, G.: 'Optical design of evanescently coupled, waveguide fed photodiodes for ultrawide-band applications', *IEEE Photonics Technol. Lett.*, 1999, **11**, (1), pp. 111–113

8 MAGNIN, V., GIRAUDET, L., HARARI, J., DECOBERT, J., PAGNOT, P., BOUCHEREZ, E., and DECOSTER, D.: 'Design, optimisation and fabrication of side illuminated PIN photodetectors with high responsivity and high alignment tolerance for 1.3 μm and 1.55 μm wavelength use', submitted to *J. Lightwave Technol.*

Two-dimensional smart detector array for interferometric applications

S. Bourquin, P. Seitz and R.P. Salathé

A 58 × 58 pixel CMOS detector array for on-chip amplitude demodulation on all pixels in parallel is presented. Optical signals can be detected at Doppler frequencies of 1 kHz up to 1 MHz, with a dynamic range of 57 dB, and at a pixel readout rate of up to 3 MHz.

Introduction: In interferometry, the amplitude and phase of the interference signal often have to be retrieved within a high DC level of background light. In singlemode systems, e.g. fibre interferometers, lock-in detection schemes fulfil this task in an appropriate way. In bulk interferometers, charge-coupled device (CCD) cameras are usually used with off-chip signal processing for amplitude demodulation [1 – 3]. These methods suffer from the following disadvantages: (i) the modulation frequency must be known precisely, (ii) off-chip electrical or software signal conditioning is necessary to extract the information on the amplitude modulation, (iii) averaging is needed to improve the signal-to-noise ratio, which significantly increases the measurement time and (iv) the DC light offset limits the dynamic range of the CCD camera.

Here, we propose to overcome these disadvantages with a novel two-dimensional CMOS camera based on the concept of 'smart pixels' [4]. All pixels perform detection and amplitude demodulation of the optical signals on-chip and in parallel without signal sampling. The modulation amplitude is directly read out of the sensor, one pixel after the other. No additional signal processing is necessary. This approach enables detection at high speed and sensitivity with a performance close to the shot noise limit.

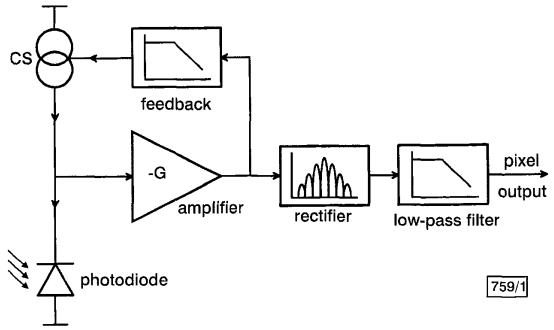

Fig. 1 *Block diagram of one pixel*

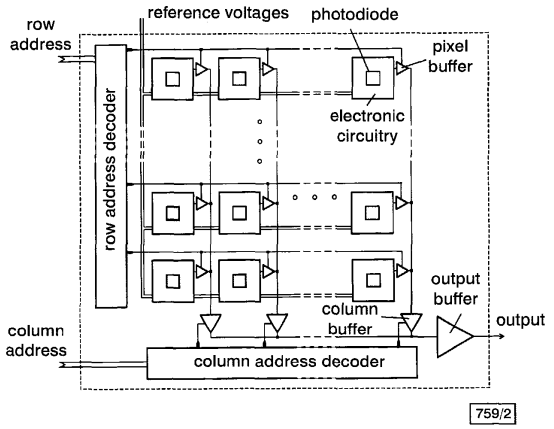

Fig. 2 *Schematic diagram of two-dimensional detector array architecture with individual pixel cells, decoder and buffer modules*

Circuit principle: A block diagram of one pixel is shown in Fig. 1. The optical signal is detected by a photodiode, which converts the optical power into an electrical current. This photodiode is connected in series to a voltage controlled current source. The difference between the current set by the current source and the current flowing through the photodiode is amplified by a transimpedance amplifier. The voltage signal at the output of the amplifier is sent back to the feedback block that controls the current source. The tasks of the feedback loop are to keep the amplifier at its operating point and to select the frequency range for amplification. In our case, the feedback consists of a first-order lowpass filter. When the amplified signal is modulated at frequencies lower than the cutoff frequency, the lowpass filter is transparent and the feedback loop is closed. Such modulations are fully compensated by the current source that follows and the current at the input of the amplifier is kept constant. The gain at modulation frequencies smaller than the cutoff frequency is thus negligible. When the optical signal is modulated at frequencies higher than the cutoff of the lowpass filter, the filter suppresses the signal and the feedback loop is open. In this case the signal is amplified by a factor equal to the gain G of the amplifier. The modulated signal at the output of the amplifier is rectified, and the signal is filtered by the lowpass filter. Here, the cutoff frequency is chosen so that the rectified signal is integrated to give the envelope of the signal.